NEUTRON SPECTROSCOPY OF SUPERCONDUCTING FULLERIDES

KOSMAS PRASSIDES*, CHRISTOS CHRISTIDES*, JOHN TOMKINSON**,
MATTHEW J. ROSSEINSKY***, D. W. MURPHY***, AND ROBERT C. HADDON***
*School of Chemistry and Molecular Sciences, University of Sussex, Brighton BN1 9QJ, UK
**Rutherford Appleton Laboratory, Didcot, Oxon OX11 0QX, UK
***AT&T Bell Laboratories, Murray Hill, NJ 07974

ABSTRACT

The phonon spectra of pristine fullerene, superconducting K_3C_{60} and saturation-doped Rb_6C_{60} measured by inelastic neutron scattering in the energy range 2.5 - 200 meV at low temperatures reveal substantial broadening of five-fold degenerate H_g intramolecular vibrational modes both in the low-energy radial and the high-energy tangential part of the spectrum. This provides strong evidence for a traditional phonon-mediated mechanism of superconductivity in the fullerides but with an electron-phonon coupling strength distributed over a wide range of energies (33-195 meV) as a result of the finite curvature of the fullerene spherical cage.

INTRODUCTION

Early efforts in fullerene research focussed in characterising the materials and confirming the originally proposed structures [1]: truncated icosahedral (I_h) for C_{60} and ellipsoidal (D_{5h}) for C_{70}. At room temperature, solid C_{60} adopts a face-centred cubic crystal structure. At low temperatures (T<260 K), it crystallises in a simple cubic structure ($Pa3$) [2]; as a result of van der Waals interactions and electrostatic repulsions, the most electron-deficient regions of the cages (pentagonal faces) face the most electron-rich ones (the higher bond-order inter-pentagon bonds) of adjacent molecules. Synthesis of numerous derivatives soon led to many novel properties. For instance, intercalation of solid C_{60} with electron donors, like the alkali metals, leads to metallic compositions, which become superconducting [3] at T_c as high as 33 K, surpassed only by the high T_c superconducting cuprates.

In this paper, we summarize recent inelastic neutron scattering studies on solid C_{60} and the alkali-metal doped fullerides K_3C_{60} and Rb_6C_{60}. More extensive reviews of neutron scattering studies on fullerenes are in press [5,6]. A plethora of additional features to those observed by optical spectroscopy is revealed. Such knowledge of the vibrational properties of C_{60}^{n-} (n=0,3,6) is very important for both the theoretical description of their electronic structure and the implications towards the possible mechanism for superconductivity in the fullerides, providing evidence for or against the participation of phonons in the pairing interaction.

EXPERIMENTAL

The dynamical behaviour of solids gives rise to inelastic neutron scattering; the nuclei gain or lose energy when neutrons collide with them and such energy is transferred from or to

Mat. Res. Soc. Symp. Proc. Vol. 270. ©1992 Materials Research Society

crystal vibrations. Both the exchange of energy, hω and momentum, hQ can be followed:

$$h\omega = E - E' \quad ; \quad \mathbf{Q} = \mathbf{k} - \mathbf{k}' \qquad (1)$$

where **k** and **k'** are the wavevectors of incident and scattered neutrons, E and E' are the initial and final neutron energies, respectively, and **Q** is the scattering vector. IR and Raman spectroscopies are characterised by excellent energy resolution; however, they are confined to modes close to the Brillouin zone centre (**k'** = **k**, **Q** = 0). In neutron spectroscopy, even though the energy resolution is poorer, information across the Brillouin zone is obtained routinely and the observed intensities may be related to atomic displacements in a straightforward manner. Furthermore, no selection rules are present so that optically inactive modes are also observed. For a simple harmonic isotropic oscillator, the scattering law is given by:
$S(Q,\omega)=(Q^2U^2)\exp(-Q^2U^2)$, with the mean square displacement of the oscillator given by: $U^2=(\hbar/2\mu\omega)$ and μ the reduced mass and ω the fundamental frequency.

INS spectra of C_{60}, K_3C_{60} and Rb_6C_{60} at low temperatures were recorded in the energy range 2.5-200 meV (1 meV=8.066 cm^{-1}) on the time-focused crystal analyser spectrometer (TFXA) at ISIS, UK (instrumental resolution, $\Delta\omega/\omega$=2%). TFXA uses a low final neutron energy (E'=4 meV) leading to $Q^2 \propto \omega$. The consequence of the instrumental characteristics is that even for principally coherent scatterers like carbon, the incoherent approximation may be used for energy transfers $h\omega$>25 meV; however, at high energy transfers (>150 meV), the resulting Debye-Waller factors are so large that they tend to wash out some of the vibrational features.

RESULTS AND DISCUSSION

The vibrational spectra of C_{60} and its reduced forms, C_{60}^{3-} and C_{60}^{6-} are extremely rich in structure (Fig. 1). There are 174 intramolecular modes giving rise to 46 fundamentals; four are infrared active (T_{1u}) and ten are Raman active (A_g, H_g), leaving 32 optically inactive modes. INS measurements are not restricted by the usual optical selection rules and consequently, the full vibrational spectrum of C_{60}^{n-} (n=0, 3, 6), may be recorded. In addition, there is information on the intermolecular (external) low-energy modes. The intramolecular modes are not expected to show significant dispersion, permitting direct comparisons between the INS data and the available zone-centre theoretical and experimental data to be made.

The vibrational spectra [6-10] may be divided into two principal regions : 0-30 meV (lattice modes) and 30-210 meV (intramolecular modes). There is an energy gap of the order of ≈10-15 meV separating inter- from intramolecular modes. The intramolecular part of the spectrum extends smoothly from 30 to 210 meV. C_{60} lacks a central atom and consequently, radial forces are weak and the cage vibrations may be distinguished into radial (≈30-110 meV) and tangential (≈110-200 meV) ones. As a result of the carbon cage reduction $C_{60} \rightarrow C_{60}^{3-} \rightarrow C_{60}^{6-}$, the high energy cut-off in the vibrational DOS softens substantially from 205.0 meV through 198.0 meV (3.4%) to 190.2 meV (7.2%), whereas the low-energy onset is barely affected, showing a hardening (0.8 meV) for C_{60}^{6-}; this reflects the pronounced effect of reduction on the vibrational modes involving substantial stretching components, particularly of the high π-order six-six ring fusions. Table 1 summarizes positions and (tentative) assignments of some vibrational modes.

TABLE I. Vibrational spectra of C_{60} (20 K), K_3C_{60} (5 K) and Rb_6C_{60} (20 K) with tentative assignments. All energies are given in meV (1 meV=8.066 cm^{-1}). Asterisks denote optically active (IR, Raman) vibrational modes. Assignments of the optically inactive modes were made using the results of the quantum chemical calculations of Negri et al. [11].

Assignment	C_{60} [6]	K_3C_{60} [7]	Rb_6C_{60} [8]
Lattice modes	12.0, 18.0	4.3, 14.0	6.4, 8.4, 13.1
$H_g^{(1)}$*	33.1	32.7	33.9
T_{2u}, G_u	42.7, 44.3	43.7	43.7
H_u	50.0	49.2	46.6
$H_g^{(2)}$*	53.2	52.5	53.1
G_g, A_g*	60.3	59.9	59.1
T_{1u}*, G_g (?)	66.1	63.6, 68.5	66.7, 68.2
T_{1g}, H_u (?), T_{1u}*	(68.6), 70.7	71.6	71.2
T_{2u}(?)	83.4	81.4	82.7
$H_g^{(3)}$*	88.2	86.5	85.9
H_u(?)	91.9	—	—
$H_g^{(4)}$*	96.2	94.0	—
Energy cut-off	205.0	198.0	190.2

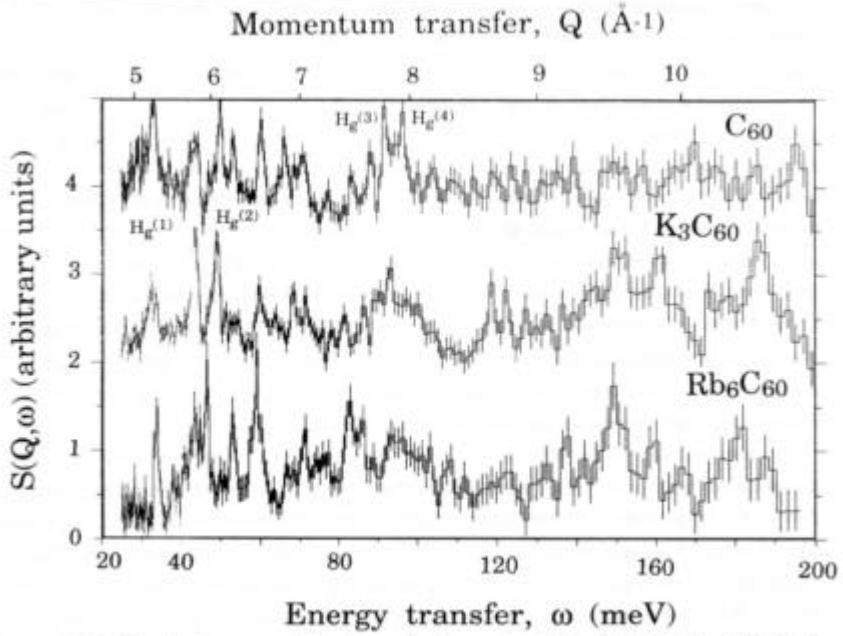

Figure 1. INS vibrational spectra of the intramolecular modes of C_{60} (20 K), K_3C_{60} (5 K) and Rb_6C_{60} (20 K) in the energy region 25-200 meV.

Phonon modes are well separated in the low-energy (30-90 meV) range and changes in position and width can be followed with confidence as a function of the reduction level of the fullerene cage. The molecular nature of the superconducting fullerides results in fairly dispersionless phonon branches, and consequently, the electron-phonon Hamiltonian [12,13] has a particularly simple form. The total electron-phonon coupling constant λ is simply expressed as a sum of partial contributions λ_ν, associated with the each mode ν mediating the pairing interaction, $\lambda = \sum_\nu \lambda_\nu$. This is further simplified if we focus on the t_{1u} electronic states which are occupied on electron-doping of C_{60}. Using simple symmetry arguments [12,13], it can be shown that in icosahedral symmetry the only relevant intramolecular modes that couple to the t_{1u} conduction electrons ($t_{1u} \otimes t_{1u} = A_g \oplus T_{1g} \oplus H_g$) are of H_g symmetry, while the totally symmetric A_g modes become active only for finite wavevectors ($Q \neq 0$). Strong electron-phonon coupling should produce substantial broadening and softening of the affected intramolecular H_g modes in the superconducting fullerides, compared to pristine C_{60}. Quantitatively such effects on the position and width may be estimated using the expressions:

$$\Delta\omega_\nu = -(\lambda_\nu/5)\,\omega_\nu \quad ; \quad \gamma_\nu = (\pi/5)\,N(\varepsilon_F)\,\lambda_\nu\,\omega_\nu^2 \qquad (2)$$

where $\Delta\omega_\nu$ is the change in frequency upon reduction to C_{60}^{3-} and γ_ν is the increase in full-width at half-maximum of the five-fold degenerate νth phonon.

The INS data provide evidence of strong electron-phonon coupling to the H_g modes. Indeed the most remarkable feature when comparing the K_3C_{60} and C_{60} INS spectra is the virtual disapperance, due to a 4.3 meV increase in FWHM, of the $H_g^{(2)}$ mode at 53.2 meV, consistent with strong electron-phonon coupling (Table 2). Using eq (2), we find an electron-phonon coupling constant for this mode of $\lambda^{(2)} \approx 0.17$, approximately 30% of the total λ. Note that by coincidence the $H_g^{(2)}$ mode occurs in a region of the spectrum where there are no neighbouring or overlapping peaks, making our conclusions on the effects of doping on its width and position *unambiguous*. The dominant rôle of this mode has also been confirmed by Raman studies on ultrathin Rb_xC_{60} (x=0-3) films [15]. Strong coupling is also evident for the well-separated $H_g^{(1)}$ mode which broadens by 1.0 meV, resulting in an estimated $\lambda^{(1)}$ contribution to the total λ of 0.10; Raman studies also show that this mode shows a Fano lineshape [16]. $H_g^{(4)}$ is more weakly coupled and we estimate an increase in γ of >3.1 meV, corresponding to a lower limit for $\lambda^{(4)}$ of 0.04. $H_g^{(3)}$ shows a virtually unchanged FWHM, even though it is somewhat softer. Information on the λ_ν's may be also extracted through the softening of phonon frequencies due to electron-phonon coupling, eq (2). However, *changes in phonon linewidths are more reliable measures of electron-phonon interactions* as energy changes also arise as a result of the cage reduction and depend on details of the electronic structure of the cluster.

Interpretation of the INS spectra in the tangential-mode regime (120-200 meV) is not unambiguous because of both a worsening in resolution and a substantial intensity attenuation due to the large Debye-Waller factors. Furthermore, broadening scales with ω^2, making identification of the affected phonons very difficult. Nonetheless, we can see that $H_g^{(8)}$ should couple strongly as there is in K_3C_{60} a hole in the spectrum at the position where it was observed for C_{60}. A definitive statement about the effect of intercalation on the $H_g^{(5\text{-}7)}$ modes at 136, 155 and 177 meV in C_{60} is difficult because they are weak, and there are significant changes in the

TABLE II. Observed positions, ω_v of the four radial H_g modes in C_{60} and their broadenings, γ_v on reduction to C_{60}^{3-} together with calculated electron-phonon coupling strengths, V_v in meV for a density-of-states N(0)=14 states/eV/spin/C_{60}. We also include for comparison the values of γ_v, estimated by the LDA frozen phonon calculations of Schluter et al.[12].

Vibrational mode	$H_g^{(1)}$	$H_g^{(2)}$	$H_g^{(3)}$	$H_g^{(4)}$
ω_v / meV	33.1	53.2	88.1	96.2
γ_v / cm^{-1}	8	35	1	25
$\gamma_{v\text{-calc}}$ / cm^{-1}	7	15	23	56
V_v / meV	7.4	12.4	0.1	2.7

spectra of K_3C_{60} in these regions. However, our experimental results uniquely confirm the important conclusion that electron-phonon coupling strength should be distributed between both buckling and tangential modes. Using the LDA frozen-phonon calculated λ_v values of Schluter et al.[12] for the tangential and combining it with our estimates for the radial modes, we find

$$\lambda=0.64.$$

This may be combined with estimates of the density-of-states N(0)=14 states/C_{60}/eV/spin and the Coulomb pseudopotential $\mu^*=0.15$ [17] to give, using McMillan's formula,

$$T_c = \frac{\omega_{log}}{1.2}\exp\left[-\frac{1.04\,(1+\lambda)}{\lambda-\mu^*(1+0.62\lambda)}\right] \qquad (3)$$

an estimate of T_c=17 K (for ω_{log}=1072 K), in good agreement with the experimentally observed values. A crucial point revealed by our results is the contrast with alkali-intercalated graphite, where the corresponding buckling modes do not couple to the π electrons because of symmetry restrictions. It appears that coupling to the radial modes, because of the finite curvature of the fullerene cage [12], accounts for roughly half the total electron-phonon coupling strength in K_3C_{60} and leads to a substantially increased T_c, compared to the lamellar graphite intercalates.

Further insight into the origin of phonon broadening in K_3C_{60} is provided by the INS spectra of insulating Rb_6C_{60}. The $H_g^{(2)}$ mode with the strongest contribution to the total electron-phonon coupling strength reappears very sharp at 53.1 meV with only a 0.1 meV change in FWHM, compared to C_{60}. The $H_g^{(1)}$ mode, also strongly coupled, similarly sharpens substantially compared to K_3C_{60} and shows an even smaller FWHM than in C_{60}. As a result, we can exclude both K^+ disorder effects and effects due to reduction, as being responsible for the remarkable broadening of certain intramolecular modes in K_3C_{60}. Strong electron-phonon coupling is an excellent candidate for these experimental observations.

CONCLUSIONS

The unusually high T_c's observed in the superconducting fullerides can be explained without invoking any unusual or exotic interactions; the INS results are consistent with weak coupling superconductivity, in agreement with isotope-effect measurements [17] and intramolecular electron-phonon coupling theories [12,13]. Both radial and tangential vibrational modes

contribute significantly to the electron-phonon coupling strength, as a result of the curvature of the spherical fullerene skeleton. This may be contrasted with the graphite intercalates which show much lower T_c's and no coupling is allowed by symmetry for the low-energy radial modes.

ACKNOWLEDGEMENTS

We thank J.R.D. Copley, T.J.S. Dennis, J.P. Hare, H.W. Kroto, M. Schluter, R. Taylor, D.R.M. Walton, and F. Zerbetto for valuable discussions. KP acknowledges support from the SERC and the Royal Society.

REFERENCES

1. H.W. Kroto, J.R. Heath, S.C. O'Brien, R.F. Curl, and R.E. Smalley, Nature 318, 162 (1985).
2. W.I.F. David, R.M. Ibberson, J.C. Matthewman, K. Prassides, T.J.S. Dennis, J.P. Hare, H.W. Kroto, R. Taylor, and D.R.M. Walton, Nature 353, 147 (1991); W.I.F. David, R.M. Ibberson, T.J.S. Dennis, J.P. Hare, and K. Prassides, Europhys. Lett. 18, 225 (1992).
3. A.F. Hebard, M.J. Rosseinsky, R.C. Haddon, D.W. Murphy, S.H. Glarum, T.T.M. Palstra, A.P. Ramirez, and A.R. Kortan, Nature 350, 660 (1991).
4. J.R.D. Copley, D.A. Neumann, R.L. Cappelletti, and W.A. Kamitakahara, J. Phys. Chem. Solids, in press.
5. K. Prassides, H.W. Kroto, R. Taylor, D.R.M. Walton, W.I.F. David, J. Tomkinson, M.J. Rosseinsky, D.W. Murphy, and R.C. Haddon, Carbon, in press.
6. K. Prassides, T.J.S. Dennis, J.P. Hare, J. Tomkinson, H.W. Kroto, R. Taylor, and D.R.M. Walton, Chem. Phys. Lett. **187**, 455 (1991).
7. K. Prassides, J. Tomkinson, C. Christides, M.J. Rosseinsky, D.W. Murphy, and R.C. Haddon, Nature 354, 462 (1991).
8. K. Prassides, C. Christides, M.J. Rosseinsky, J. Tomkinson, D.W. Murphy, and R.C. Haddon, Europhys. Lett, submitted.
9. R.L. Cappelletti, J.R.D. Copley, W.A. Kamitakahara, F. Li, J.S. Lannin, and D. Ramage, Phys. Rev. Lett. 66, 3261 (1991).
10. C. Coulombeau, H. Jobic, P. Bernier, C. Fabre, D. Schütz, and A. Rassat, J. Phys. Chem. 96, 22 (1992).
11. F. Negri, G. Orlandi, and F. Zerbetto, Chem. Phys. Lett. 144, 31 (1988); Chem. Phys. Lett. 190, 174 (1992).
12. M.A. Schluter, M. Lannoo, M. Needels, G.A. Baraff, and D. Tomanek, Phys. Rev. Lett. 68, 526 (1992) and unpublished work.
13. C.M. Varma, J. Zaanen, and K. Raghavachari, Science 254, 989 (1991).
14. M.G. Mitch, S.J. Chase, and J.S. Lannin, Phys. Rev. Lett. 68, 883 (1992).
15. P. Zhou, K.A. Wang, A.M. Rao, P.C. Eklund, G. Dresselhaus, and M.S. Dresselhaus, unpublished.
16. A.P. Ramirez et al., Phys. Rev. Lett. 68, 1058 (1992); C.C. Chen and C.M. Lieber, J. Am. Chem. Soc. in press.